HHS Public Access

Author manuscript

Neuroscience. Author manuscript; available in PMC 2015 August 22.

Published in final edited form as:

Neuroscience. 2012 September 18; 220: 277–290. doi:10.1016/j.neuroscience.2012.06.019.

INTRANUCLEAR MATRIX METALLOPROTEINASES PROMOTE DNA DAMAGE AND APOPTOSIS INDUCED BY OXYGEN–GLUCOSE DEPRIVATION IN NEURONS

J. W. Hill, **R. Poddar**, **J. F. Thompson**, **G. A. Rosenberg**, and **Y. Yang***

University of New Mexico Health Sciences Center, Department of Neurology, Albuquerque, NM 87131, USA

Abstract

Degradation of the extracellular matrix by elevated matrix metalloproteinase (MMP) activity following ischemia/reperfusion is implicated in blood–brain barrier disruption and neuronal death. In contrast to their characterized extracellular roles, we previously reported that elevated intranuclear MMP-2 and -9 (gelatinase) activity degrades nuclear DNA repair proteins and promotes accumulation of oxidative DNA damage in neurons in rat brain at 3-h reperfusion after ischemic stroke. Here, we report that treatment with a broad-spectrum MMP inhibitor significantly reduced neuronal apoptosis in rat ischemic hemispheres at 48-h reperfusion after a 90-min middle cerebral artery occlusion (MCAO). Since extracellular gelatinases in brain tissue are known to be neurotoxic during acute stroke, the contribution of intranuclear MMP-2 and -9 activities in neurons to neuronal apoptosis has been unclear. To confirm and extend our *in vivo* observations, oxygen–glucose deprivation (OGD), an *in vitro* model of ischemia/reperfusion, was employed. Primary cortical neurons were subjected to 2-h OGD with reoxygenation. Increased intranuclear gelatinase activity was detected immediately after reoxygenation onset and was maximal at 24 h, while extracellular gelatinase levels remained unchanged. We detected elevated levels of both MMP-2 and -9 in neuronal nuclear extracts and gelatinase activity in neurons co-localized primarily with MMP-2. We found a marked decrease in PARP1, XRCC1, and OGG1, and decreased PARP1 activity. Pretreatment of neurons with selective MMP-2/9 inhibitor II significantly decreased gelatinase activity and downregulation of DNA repair enzymes, decreased accumulation of oxidative DNA damage, and promoted neuronal survival after OGD. Our results confirm the nuclear localization of gelatinases and their nuclear substrates observed in an animal stroke model, further supporting a novel role for intranuclear gelatinase activity in an intrinsic apoptotic pathway in neurons during acute stroke injury.

Keywords

stroke; matrix metalloproteinase; DNA repair; oxidative DNA damage; neuronal apoptosis

*Corresponding author. Address: Department of Neurology, MSC11 6035, 1 University of New Mexico, Albuquerque, NM 87131-0001, USA. Tel: +1-(505)-272-5987; fax: +1-(505)-272-6692. yyang@salud.unm.edu (Y. Yang).

CONFLICT OF INTEREST

The authors declare no conflict of interest.

INTRODUCTION

Cerebral ischemia induces neuronal death primarily by necrosis in the ischemic core, while loss of neurons in less severely affected penumbral tissue surrounding the infarct core occurs by apoptosis over hours to days (Broughton et al., 2009). Characterization of apoptotic pathways in ischemic neurons may allow for therapeutic targeting and prevention of apoptosis in the penumbra, thereby limiting the evolution of infarct volume and improving outcome after stroke. Neuronal death during the acute phase of ischemic stroke is mediated by early activation of matrix metalloproteinases (MMPs), which exert neurotoxic effects both by degradation of the extracellular matrix leading to anoikis and by opening of the blood–brain barrier (BBB) resulting in hemorrhagic damage and infiltration of inflammatory cells at the infarct site (Gu et al., 2002; Cunningham et al., 2005; Rosenberg and Yang, 2007; McColl et al., 2008; Candelario-Jalil et al., 2009; Jin et al., 2010). Although initially thought to act primarily on extracellular targets, recent studies have revealed that MMPs are also localized to various intracellular sites, including the nucleus (Kwan et al., 2004; Yang et al., 2007, 2010; Amantea et al., 2008; Ali and Schulz, 2009; Cuadrado et al., 2009; Wakisaka et al., 2010; Gueye et al., 2011; Mannello and Medda, 2012). Intracellular substrate proteolysis by MMPs is involved in innate immune defense and apoptosis and influences oncogenesis and the pathology of cardiac, neurological, protein conformational, and autoimmune diseases (Cauwe and Opdenakker, 2011; Mannello and Medda, 2012). MMP-2, -3, -9, -13, and membrane-type 1 MMP (MT1-MMP) have all been identified in neuronal nuclei and gelatinases (MMP-2 and -9) and MMP-3 have been implicated in the progression of infarct volume and neuronal death in animal models of stroke (Gasche et al., 2001; Gu et al., 2005; Si-Tayeb et al., 2006; Yang et al., 2007, 2010; Amantea et al., 2008; Cuadrado et al., 2009). In these studies, MMP inhibitors have been shown to be neuroprotective, suggesting a role for MMPs in cell death. However, the mechanisms by which intracellular gelatinases may promote neuronal injury remain largely uncharacterized.

Neuronal apoptosis by anoikis after ischemic injury has been proposed as a mechanism of cell death due to the action of extracellular gelatinase activity on the extracellular matrix (Gu et al., 2002). Studies have proposed that MMPs may mediate neuronal death by pro-apoptotic signaling upstream of caspases, potentiating neuroinflammation through processing of IL-1β in ischemic cortex, or through the activation of calpains in ischemic brain (Copin et al., 2005; Amantea et al., 2007; Choi et al., 2008). Our recent study identified the first molecular targets of nuclear gelatinase activity in ischemic neurons and provided additional clues as to how intracellular gelatinases may facilitate neuronal death during ischemia/reperfusion (Yang et al., 2010). Two nuclear proteins, poly-ADP ribose polymerase (PARP1), a protein central in DNA damage sensing and signaling, cell death pathway initiation, and DNA base excision repair (BER), and X-ray cross-complementary factor 1 (XRCC1), an essential scaffolding protein in BER, were shown to be degraded by nuclear gelatinases in a rat stroke model and were confirmed as substrates of MMP-2 and -9 using recombinant proteins *in vitro* (Yang et al., 2010). PARP1 and XRCC1 are critical in the repair of oxidative DNA damage, including abasic (AP sites) and 8-hydroxy-2′-dexoguanine (8-oxo-dG), which if left unrepaired or incompletely repaired, are cytotoxic and promote neuronal death. In this transient middle cerebral artery occlusion (MCAO)

model, degradation of PARP1 and XRCC1 by MMP-2 and -9 was shown to be associated with elevated oxidative DNA damage which may in turn promote apoptosis. Furthermore, in rats treated with an MMP inhibitor, there was a significant reduction in the degradation of PARP1 and XRCC1 that was accompanied by a reduction in oxidative DNA damage levels at 3-h reperfusion (Yang et al., 2010). Based on these results, we hypothesized that intranuclear MMP-2 and -9 may facilitate neuronal apoptotic death via their proteolysis of nuclear DNA repair proteins after stroke injury. However, in an animal model, BBB opening, glial cells, which are a significant source of MMPs, and the inflammatory response all contribute to neuronal death are not easily separated from intrinsic neuronal cell death pathways which may involve intranuclear MMP activity. Accordingly, further studies have been necessary to determine the contribution of intracellular MMP activity to ischemic neuronal apoptosis.

In the present study, to test the hypothesis that intracellular MMPs mediate neuronal apoptotic death, we first examined the contribution of MMPs to neuronal apoptosis in a transient MCAO model in rats. Then, using an oxygen–glucose deprivation (OGD) model of stroke in primary cortical neurons, we investigated the roles of MMP-2 and -9 nuclear localization and activity in neuronal apoptosis during reoxygenation.

EXPERIMENTAL PROCEDURES

MCAO with reperfusion

The study was approved by the University of New Mexico Animal Care Committee and conformed to the National Institutes of Health Guidelines for use of animals in research. Male spontaneously hypertensive rats (SHR), weighing 300–320 g, were anesthetized with 2% isoflurane in 1 L/min oxygen. Ninety minutes MCAO was done by inserting an intraluminal nylon suture with a bulb at the end as previously described (Rosenberg et al., 2001; Yang et al., 2010). Reperfusion was achieved by slowly removing the suture after occlusion. To investigate the effects of MMP inhibition on neuronal apoptotic death, rats received either vehicle (saline) or the MMP inhibitor BB-1101 (British Biotech Pharmaceuticals, Oxford, UK) given intraperitoneally at a dose of 30 mg/kg body weight 10 min before the start of MCAO. Sham animals underwent insertion of an intraluminal suture which was immediately removed.

Stereology of TUNEL positivity in ischemic hemispheres

Brain tissues were fixed with 2% paraformaldehyde, 0.1 M sodium periodate, 0.075 M lysine in 100 mM phosphate buffer at pH 7.3 (PLP). Terminal deoxynucleotidyl transferase-mediated dUTP nick end labeling (TUNEL) assay was performed on brain sections to identify apoptotic cells with DNA fragmentation using the NeuroTACS II kit (Trevigen, Gaithersburg, MD, USA) according to the procedure specified by the manufacturer. Briefly, 20-μm fixed rat brain sections were rehydrated and incubated overnight with NeuroPore permeabilization agent at 4 °C. Endogenous peroxidases were quenched with 0.3% hydrogen peroxide in methanol. Slides were then incubated with the labeling reaction mixture for 1 h at 37 °C. Slides were incubated in reaction stop buffer, Vectastain Elite ABC reagents (Vector Laboratories, Burlingame, CA, USA), reacted with 3,3′-diaminobenzidine

(DAB) to allow visualization of immunolabeling, and counterstained with Cresyl Violet acetate (CVA, Sigma–Aldrich, St. Louis, MO, USA). For positive controls, the provided nuclease was added to the labeling reaction mix to induce TUNEL positivity in all cells. As a negative control, slides were prepared in a labeling reaction mix without the terminal deoxynucleotidyl transferase enzyme resulting in no TUNEL positivity (data not shown). Unbiased stereology was performed using StereoInvestigator software (Version 6, MBF Bioscience, Williston, VT, USA) controlling a motorized stage-equipped Olympus BX-51 microscope (Olympus America Inc., Center Valley, PA, USA) (Walker and Rosenberg, 2010; Yang et al., 2011). Employing the optical fractionator function of StereoInvestigator, we counted TUNEL-positive cells in ischemic hemispheres with 48-h reperfusion. The area of stereological analysis encompassed the entire ischemic hemisphere over a distance of 3.0, 1.5 mm rostral and caudal to the bregma. Tissue sections were blinded to the investigator as to animal identity. For dual-immunofluorescence, TUNEL-labeled brain sections were incubated with neuron-specific NeuN primary antibody overnight followed by streptavidin-conjugated fluorescein isothiocyanate (FITC) and Cyanine 3 (Cy3)-conjugated secondary antibody. 4′-6-diamidino-2-phenylindole (DAPI) (Life Technologies, Grand Island, NY, USA) was used to label cell nuclei. All slides were viewed on an Olympus BX-51 bright field and fluorescence microscope equipped with an Optronics digital camera. Dual-immunofluorescence slides were also imaged using highresolution confocal microscopy to verify co-localization of antigens (Zeiss LSM 510, Carl Zeiss Microscopy, Thornwood, NY, USA).

Primary cortical neuron culture

Cortices from Sprague–Dawley rat embryos at day 18 of gestation were triturated and trypsinized for 10 min in phosphate-buffered saline (PBS) containing 0.025% trypsin–EDTA (Life Technologies). Digestion was stopped by addition of DMEM containing 10% fetal bovine serum (FBS). Trypsinized cells were filtered using sterile 70-μm disposable cell filters (Becton–Dickinson, Franklin Lakes, NJ, USA), centrifuged at 700*g*, aspirated, and washed twice with Neurobasal medium containing 2% FBS (Life Technologies). Mixed cortical cells in Neurobasal 2% FBS were preplated 4 times for 30 min in 150-mm vacuum plasma-treated tissue culture dishes without poly-D-lysine coating (Becton–Dickinson). During these preplating steps, primarily non-neuronal cells, including endothelial cells, microglia, and astrocytes selectively adhere to the culture dish, thereby enriching the neuronal population. Following preplating, cells were washed in Neurobasal 2% FBS, suspended in Neurobasal 2% FBS, and counted. Cells were plated in poly-D-lysine-coated dishes or, for immunocytochemistry, in 24-well dishes containing poly-D-lysine-coated 12-mm-diameter glass coverslips (Carolina Biological Supply Company, Burlington, NC, USA) at 50×10^3 cells/cm^2. Twenty-four hours later (1 day *in vitro*, DIV), medium was changed 50% with Neurobasal 2% B27 (Life Technologies). At 2 DIV, cultures were treated with 4 μM cytosine arabinoside (AraC) (Sigma–Aldrich). At 4 and 8 DIV, cells were fed 50% Neurobasal 2% B27. Experiments were performed at 12 DIV at which time cultures were ~98% neurons as determined by microtubule-associated protein 2 (MAP2) staining and analysis by flow cytometry (data not shown).

Oxygen and glucose deprivation

Cortical neurons were deprived of oxygen and glucose by incubation in deoxygenated glucose-free Hank's buffered saline solution (HBSS). HBSS was prepared as follows: sodium chloride, NaCl, 8.0 g/L, potassium chloride, KCl, 0.4 g/L, potassium phosphate monobasic, KH_2PO_4, 0.06 g/L, sodium phosphate dibasic, Na_2HPO_4, 0.048 g/L, magnesium sulfate, $MgSO_4$, 0.098 g/L, calcium chloride, $CaCl_2$, 0.14 g/L, sodium bicarbonate, $NaHCO_3$, 0.35 g/L, D-glucose, $C_6H_{12}O_6$, 1.0 g/L. Solutions were adjusted to pH 7.4 and sterilized by vacuum filtration through 0.2-μm polyether sulfone (PES) membranes. Glucose-free HBSS was prepared by omitting glucose and adding an additional half molar amount of NaCl to adjust osmolarity (8.162 g/L NaCl). Glucose-free HBSS was deoxygenated in a gas washing bottle with 95% nitrogen, 5% CO_2 for 1 h at a flow rate of 1 L/min in a 37 °C water bath. Culture dishes were washed twice with deoxygenated glucose-free HBSS and placed in a modular incubator chamber (Billups-Rothenberg, Inc., Del Mar, CA, USA) at 37 °C. The chamber was then flushed with 95% nitrogen, 5% CO_2 for 30 min at a flow rate of 3 L/min and sealed for 1.5 h (2 h OGD). Normoxic control cells were handled identically but were incubated in a 5% CO_2 incubator with normal HBSS pre-equilibrated in a 5% CO_2 atmosphere overnight. MMP-2/MMP-9 inhibitor II, (2R)-[(4-Biphenylylsulfonyl)amino]-N-hydroxy-3-phenylpropionamide (EMD Millipore, Billerica, MA, USA), a cell-permeable and selective inhibitor of MMP-2 and -9, was dissolved in dimethyl sulfoxide (DMSO) as a 10 mM stock solution and stored in aliquots at −20 °C. The stock solution was serially diluted to 1 μM in glucose-free HBSS and added to cultures 1 h before OGD (1 nM final concentration). Untreated cells received DMSO vehicle diluted in glucose-free HBSS. Pretreatment medium with or without added inhibitor was saved and replaced after OGD was performed in glucose-free HBSS with or without 1 nM MMP inhibitor. Control cultures exposed to mock OGD in CO_2-equilibrated normal HBSS were similarly treated with MMP inhibitor as indicated.

Cell extracts and Western blot

Nuclear extracts were prepared from primary neurons using NEPER reagents (Thermo Fisher Scientific, Rockford, IL, USA) according to the manufacturer's instructions. Protein concentrations were determined using the Pierce BCA (bicinchoninic acid) Protein Assay. Protein samples were heated at 95 °C for 5 min in 1× Laemmli sample buffer and electrophoresed on 4–20% polyacrylamide gels (Bio-Rad Laboratories, Hercules, CA, USA). Separated proteins were transferred to polyvinylidene fluoride (PVDF) membranes (EMD Millipore) and specific proteins were detected using antibodies against PARP1 (Cell Signaling Technology, Inc., Danvers, MA, USA), XRCC1 (Sigma–Aldrich), 8-oxoguanine DNA glycosylase 1 (OGG1) (Novus Biologicals, Littleton, CO, USA), and apurinic/apyrimidinic (AP) DNA endonuclease 1 (APE1) (Novus Biologicals). Quantification of protein levels was performed by densitometry using ImageJ software and normalized to total protein as measured by Coomassie staining of PVDF membranes.

In situ and gelatin zymography

In situ zymography (ISZ) was performed as described previously (Yang et al., 2010) with modifications. Briefly, cultured neurons on coverslips were washed in PBS and incubated in

20 μg/ml DQ Gelatin (EnzCheck Gelatinase/Collegenase Assay kit, Life Technologies) for 10 min at 37 °C. Cells were washed twice with PBS, fixed with 4% paraformaldehyde for 30 min at room temperature, and either stained with DAPI and mounted on slides with Fluromount (Sigma–Aldrich) or further processed with immunocytochemistry. Gelatin zymography was performed as previously described (Asahi et al., 2000).

Immunocytochemistry

After fixation in 4% paraformaldehyde for 30 min, neurons grown on coverslips were blocked and permeabilized for 30 min in PBS containing 1% BSA, 0.1% Tween 20. Cells were incubated with MAP2 (Cell Signaling Technology, Inc.), MMP-2 (EMD Millipore), or MMP-9 (EMD Millipore) antibodies (1:2000) in PBS containing 1% BSA, 0.01% Tween 20 for overnight at 4 °C. Coverslips were washed 3× in PBS, 1% BSA, 0.01% Tween 20, and incubated with FITC- or Cy3-conjugated secondary antibody (1:2000, Life Technologies) for 1 h at room temperature. Coverslips were washed 3× in PBS, 1% BSA, 0.01% Tween 20, DAPI stained to visualize nuclei, and mounted on slides.

TUNEL assay in primary neurons

Apoptosis was measured in primary neurons using an APO-DIRECT apoptosis kit (EMD Millipore). The assay was adapted for adherent cells attached to 12-mm-diameter coverslips. Cells were stained with DAPI and scored for apoptosis. For co-localization of TUNEL with ISZ, APO-DIRECT FITC-conjugated deoxyuridine triphosphate (dUTP) was substituted with biotinylated dUTP (Trevigen) and detected with Cy3-streptavidin (Life Technologies).

DNA damage and PAR assays

Genomic DNA was prepared from primary neurons following 24-h reoxygenation after OGD using DNAzol reagent (Life Technologies) according to the manufacturer's instructions. Oxidative DNA damage (8-hydroxy-2′-deoxyguanine or 8-oxo-dG) in genomic DNA was measured using an OxiSelect Oxidative DNA Damage ELISA kit (Cell Biolabs, Inc., San Diego, CA, USA) and 1 μg of genomic DNA according to the manufacturer's instructions. Poly ADP-ribose (PAR) was measured in nuclear extracts of primary neurons using a PARP *In Vivo* Pharmacodynamic Assay II kit (Trevigen) and 1 μg of nuclear extract according to the manufacturer's instructions.

Statistical analysis

Statistical significance of differences between groups among repeat experiments was evaluated by one-way ANOVA and Bonferroni's multiple comparison test using GraphPad Prism 5 software (GraphPad Software, Inc., La Jolla, CA, USA). In all statistical tests, differences were considered significant when $p < 0.05$. Data are presented as means with standard deviation.

RESULTS

Neuronal apoptotic cell death is associated with early MMP activation *in vivo*

To determine the contribution of MMPs to brain cell apoptosis, we performed TUNEL staining in rat brains subjected to 90-min MCAO followed by 48-h reperfusion with or without treatment with broad-spectrum MMP inhibitor BB-1101. We detected TUNEL-positive cells in ischemic hemispheres of both BB-1101- and vehicle-treated rat brains at 48-h reperfusion (Fig. 1). In infarcted areas of cortex, caudate, and piriform cortex (as indicated in Fig. 1d inset), fewer TUNEL-positive cells were seen in ischemic hemispheres treated with BB-1101 compared to vehicle (Fig. 1a–c). We then counted the TUNEL-positive cells in ischemic hemispheres over a total distance of 3.0 mm from 1.5 mm rostral and caudal to the bregma using an unbiased stereological method (Walker and Rosenberg, 2010; Yang et al., 2011). The number of TUNEL-positive cells was normalized by edema index (data not shown) at 48-h reperfusion. This analysis revealed that the number of TUNEL-positive cells significantly increased at 48 h in ischemic hemispheres of the vehicle- and BB-1101-treated groups compared with sham-operated animals (Fig. 1d). Treatment with BB-1101 significantly reduced the number of TUNEL-positive cells in the ischemic hemisphere compared with the vehicle-treated group (Fig. 1d). To determine if the TUNEL-positive cells are neurons, TUNEL-labeled brain sections were double-immunostained for NeuN, a neuronal marker. Confocal microscopy demonstrated that most TUNEL-positive cells in ischemic hemispheres were co-localized with NeuN immunostaining at 48-h reperfusion (Fig. 1e). These results indicate that early increased MMP activity is involved in delayed neuronal apoptotic death after stroke.

Induction of nuclear gelatinase activity in primary neurons following OGD

To further characterize the contribution of intranuclear MMP-2 and -9 to ischemia-induced neuronal apoptosis, we moved from our *in vivo* study to an *in vitro* ischemic model using pure primary cortical neuron cultures. We first established the temporal profile of gelatinase activation induced by OGD in neurons. Gelatinase activity in primary neuronal cultures was assayed by ISZ after 2-h OGD and reoxygenation over a period of 0–24 h. Antibody against MAP2 was used as a marker of primary neurons. Immediately after OGD, increased gelatinase activity was observed in OGD-treated neurons compared to normoxic controls (Fig. 2a). The number of gelatinase-positive neurons increased from 0–24 h reoxygenation where a maximum of 74 ± 7% ISZ-positive cells was reached (Figs. 2a and 3b). The specific nuclear localization of gelatinase activity was observed in neurons at 24-h reoxygenation and classified into different stages (I–III) correlating with the progression of apoptosis (Fig. 2b). In normoxic control cells, minimal background nuclear proteolytic activity was detected (Fig. 2a, b, row 1). After OGD and 24 h reoxygenation, strong nuclear and diffuse cytoplasmic gelatinase activities appear and correlate with nuclear condensation and retraction of neuronal processes indicative of the onset of apoptosis (stage I) as illustrated in Fig. 2b, row 2. Further nuclear condensation and collapse of the cytoskeleton with concomitant loss of MAP2 staining (stage II) is shown in Fig. 2b, row 3. A late-stage apoptotic cell with fragmented nucleus and high levels of gelatinase activity (stage III) is shown in Fig. 2b, row 4. After 24 h reoxygenation, ISZ-positive cells were primarily stages II and III. ISZ-positive cells were nearly always MAP2 negative, as in stages II and III.

MMP-2/9 inhibitor II inhibits intranuclear MMP-2 and MMP-9 activity and nuclear localization induced by OGD

Levels of MMP-2 and -9 in neuronal nuclei following OGD were determined by ISZ together with MMP-2 or MMP-9 immunocytochemistry and confirmed by gelatin zymography (Figs. 2c, 3 and 4). In normoxic control cells, MMP-2 was present in both the neuronal cell body and nucleus (Fig. 2c), while MMP-9 was observed in the cell body but not in the nucleus (Fig. 2c). After OGD, both MMP-2 and -9 were observed in the nucleus (Fig. 2c) at 24-h reoxygenation. Significantly, MMP-2 in the nucleus co-localized with ISZ while MMP-9 showed minimal ISZ co-localization (Fig. 2c). This observation is consistent with our previous *in vivo* study showing that MMP-2 is the major source of gelatinase activity early after stroke (Yang et al., 2007). The contribution of MMP-2 and -9 to the gelatinase activity in neuronal nuclei was further investigated by ISZ (Fig. 3). Cortical neurons pretreated with MMP inhibitor (MMP-2/9 inhibitor II) and exposed to OGD in the presence of the inhibitor had significantly fewer gelatinase-positive cells compared to cells exposed to OGD without MMP inhibitor (Fig. 3). Treatment of neurons with MMP inhibitor significantly decreased the percentage of gelatinase-positive cells by roughly half after 2-h OGD and 24-h reoxygenation (Fig. 3). Addition of MMP inhibitor alone had no effect on gelatinase activity in normoxic control cells (Fig. 3). The increase in nuclear MMP-2 and -9 levels and activity was confirmed by gelatin zymography, a method commonly used to specifically measure MMP levels (Yang et al., 2010; Candelario-Jalil et al., 2011). The levels of both MMP-2 and -9 were significantly increased in neuronal nuclei after OGD (Fig. 4). More importantly, the forms of MMP-2 possessing enzymatic activity (64 and 62 kDa intermediate and activation forms, respectively) were detected by gelatin zymography of nuclear extracts of neurons exposed to OGD, and were significantly attenuated in the presence of MMP-2/9 inhibitor II, as were pro MMP-2 (68 kDa) and -9 (92 and 88 kDa) (Fig. 4).

Decreased levels of nuclear DNA repair proteins in primary neurons after OGD is inhibited by MMP-2/9 inhibitor II

We next determined the role of intranuclear MMP activity on the level of BER enzymes in nuclei of neurons subjected to OGD. The levels of 4 key nuclear DNA repair proteins in neuronal nuclear extracts were measured by Western blot following 2-h OGD and reoxygenation for 24 h (Fig. 5a). PARP1 and XRCC1 were decreased by roughly half 24 h after OGD (Fig. 5b). Addition of MMP inhibitor prevented the loss of PARP1 and XRCC1 (Fig. 5a, b. OGG1, the major oxidative DNA damage glycosylase activity, was decreased approximately fourfold 24 h after OGD (Fig. 5a, b. However, the loss of OGG1 was not significantly affected by MMP inhibitor. APE1, an endonuclease essential in the repair of abasic sites, was not significantly changed under OGD or normoxic conditions (Fig. 5a, b at 24-h reoxygenation. These results indicate significant OGD-induced decreases in major DNA repair proteins, which, in the case of PARP1 and XRCC1, appear to be gelatinase-associated. These results are consistent with our *in vivo* observations (Yang et al., 2010).

Attenuation of PARP1 activity and accumulation of oxidative DNA damage induced by OGD are prevented by MMP-2/9 inhibitor II

PAR is the product of PARP1 enzymatic cleavage of NAD^+ to nicotinamide and ADP-ribose and the conversion of ADP-ribose into polymeric units. PAR levels are therefore a direct measure of PARP1 activity. After OGD, PAR in neuronal nuclear extracts was decreased by half (Fig. 5c). The decrease in PAR level was significantly precluded by treatment with MMP-2/9 inhibitor II. This result is in agreement with the change in PARP1 enzyme observed after OGD (Fig. 5a, b. Since PARP1 and XRCC1 mediate repair of oxidative DNA damage, we next measured the level of 8-oxo-dG, a ubiquitous marker of oxidative stress, in neurons exposed to OGD at 24-h reoxygenation. Oxidative DNA damage, as measured by the level of 8-oxo-dG in genomic DNA, was elevated approximately twofold 24 h after OGD (Fig. 5d). Treatment with MMP inhibitor resulted in a significant reduction in 8-oxo-dG in genomic DNA compared to cells undergoing OGD without inhibitor treatment (Fig. 5d).

Inhibition of gelatinases protects neurons from OGD-induced apoptotic cell death

The contribution of intracellular MMPs to neuronal death cannot be separated from other factors in an animal stroke model. To address this issue, we used an *in vitro* approach and determined the impact of gelatinases on apoptosis in neuronal cultures exposed to OGD. Neuronal cell death by apoptosis after OGD was measured by TUNEL assay (Fig. 6). OGD induced significant apoptosis in neurons (Fig. 6a) and complete co-localization of ISZ and TUNEL was observed (Fig. 6b). OGD induced apoptosis in roughly 70% of cells after 24-h reoxygenation. Normoxic control cells were 5–10% apoptotic. Treatment with 1 nM MMP-2/9 inhibitor II decreased cell death after OGD by approximately 50% (Fig. 6c). These results implicate MMP-2 and -9 in neuronal apoptotic death at 24-h reoxygenation after OGD and, together with the involvement of MMP-2 and -9 in decreases in nuclear DNA repair enzymes and increased oxidative DNA damage, suggest that the increase in nuclear gelatinase proteolysis after OGD promotes nuclear accumulation of oxidative DNA damage in neurons, thereby promoting apoptotic death.

Extracellular gelatinase levels are unchanged after OGD

Since gelatinases are known to act extracellularly *in vivo* and influence neuronal survival after ischemia/reperfusion, we investigated the possibility that OGD might influence the activity of gelatinases in neuronal culture medium. Following OGD or control treatment and 24-h reoxygenation, culture medium was assayed for gelatinases by gelatin zymography (Fig. 7a). OGD or normoxic control treatment with or without MMP inhibitor produced no significant change in extracellular levels of MMP-2 or -9 (Fig. 7b, c, suggesting a lack of involvement of extracellular gelatinase activity in neuronal apoptosis at 24-h reoxygenation.

DISCUSSION

Our results show that inhibition of MMPs with broad-spectrum inhibitor BB-1101 in rat immediately before MCAO onset significantly decreased neuronal apoptosis at 48-h reperfusion. By using an OGD model of stroke in primary cortical neurons, we directly evaluated the intranuclear localization and activity of MMP-2 and -9 and the contribution of

intracellular gelatinases to DNA damage and neuronal cell death in ischemic insult. Use of a selective MMP-2/9 inhibitor in primary neurons decreased oxidative DNA damage and prevented apoptosis after OGD. Our results suggest a major role for proteolysis by nuclear gelatinases in the induction of an intrinsic neuronal apoptosis pathway independent of MMP-related extracellular matrix proteolysis.

We and others have shown the protective role of MMP inhibition in reducing both BBB permeability and neuronal injury after ischemia *in vivo* (Gasche et al., 2001; Copin et al., 2005; Gu et al., 2005; Amantea et al., 2007, 2008; Yang et al., 2007, 2010; Katsu et al., 2010). In a recent study, we reported that MMP-2 and -9 can cleave DNA repair proteins PARP1 and XRCC1 *in vivo* and *in vitro*. We found that increased intranuclear MMP-2 and -9 in ischemic neurons in MCAO rats facilitate oxidative DNA damage by cleaving PARP1 and XRCC1 at 3-h reperfusion (Yang et al., 2010). In the present study, we show that inhibition of MMPs *in vivo* decreases apoptosis in neurons in rat brain 48 h after MCAO. This suggests that in addition to their detrimental extracellular roles in BBB disruption (Yang et al., 2007), early increased MMPs in neuronal nuclei may be involved in neuronal apoptosis associated with oxidative DNA damage.

To further characterize the role of stroke-induced intranuclear MMP activity on neuronal apoptosis *in vivo*, we performed studies *in vitro* using an OGD stroke model in cultured primary cortical neurons. Significant apoptosis was induced in neurons and treatment of cells with a specific inhibitor of MMP-2 and -9 inhibited the gelatinase activity and prevented apoptosis. Importantly, cells positive for apoptosis were always gelatinase-positive. These results, together with our observation that a specific inhibitor of MMP-2 and -9 is highly neuroprotective in OGD, strongly suggest a major role for gelatinases in intrinsically initiated apoptosis in neurons. The loss of PARP1 and XRCC1 was inhibited by a selective MMP-2/9 inhibitor and confirms our *in vivo* studies indicating a role for gelatinases in the downregulation of nuclear DNA repair proteins following ischemia/reperfusion. We also observed decreased oxidative DNA damage in post-OGD neurons treated with gelatinase inhibitor. These results suggest the involvement of intranuclear neuronal gelatinases in the modulation of cellular DNA repair capacity and accumulation of potentially cytotoxic DNA damage and provide a mechanistic rationale for the observed neuroprotective effects of MMP-2/9 inhibitor II.

Significant evidence from animal studies has implicated MMP-2 and -9 in the deleterious effects of ischemia/reperfusion (Romanic et al., 1998; Asahi et al., 2000; Gu et al., 2005; Koistinaho et al., 2005; Amantea et al., 2007, 2008; Yang et al., 2007, 2010). MMP-2 is believed to be involved in early opening of the BBB, while MMP-9 induced later after stroke may be associated with prolonged BBB damage (Rosenberg and Yang, 2007; Yang et al., 2007, 2010; Candelario-Jalil et al., 2009; Liu et al., 2009; Jin et al., 2010). Polymorphonuclear leukocytes (PMNs) are a prevalent infiltrate at ischemic lesions *in vivo* (Neumann et al., 2008) and studies suggest that MMP-9 in ischemic brain may be primarily of neutrophil origin (McColl et al., 2008). Use of an MMP-2/9 inhibitor prevented laminin degradation and decreased neuronal apoptosis in transient focal ischemia in mice, presumably by inhibiting neuronal detachment from basement membrane proteins and preventing cell death by anoikis (Gu et al., 2005). *In vitro*, experiments with microglia co-

cultured with neurons demonstrate that MMP-9 produced by activated microglia is highly neurotoxic (Kauppinen and Swanson, 2005). These studies clearly indicate that production of gelatinases by non-neuronal cells in ischemic brain may potentiate neuronal death extrinsically *in vivo*. While the use of neuroprotective MMP inhibitors in these studies and others has definitively implicated gelatinases in neuronal death and ischemic damage after stroke, it has been unclear whether neuronal death associated with gelatinase induction is primarily extrinsic in nature, as has been previously reported, or also of intrinsic origin due to intracellular gelatinase activity in neurons.

In pure cortical neurons, our results show a significant increase in nuclear gelatinase levels and activity. We observed early prevalent nuclear gelatinase activity followed by diffuse cytoplasmic activity during later stages of cell death, consistent with previous reports of the cellular distribution of gelatinase activity occurring after stroke in animal models and human patients (Yang et al., 2007, 2010; Amantea et al., 2008; Cuadrado et al., 2009). Since essentially all neurons with clear nuclear condensation indicating apoptosis were stage II or III at 24-h reoxygenation, we hypothesize that stage I is a short-lived transitional phase along the OGD-induced apoptotic cell death pathway. That early-apoptotic stage I cells have intense, primarily nuclear gelatinase activity suggests that activation of nuclear gelatinases may be strongly associated with the initiation of apoptosis. Levels of MMP-2 and -9 were significantly increased in the nuclei of neurons 24 h after OGD as measured by immunocytochemistry, ISZ, and gelatin zymography. MMP-2/9 inhibitor II treatment significantly inhibited gelatinase activity and decreased the induction of nuclear MMP-2 and MMP-9 levels observed with OGD alone. These results suggest that in addition to directly inhibiting gelatinase activity, MMP-2/9 inhibitor II may also influence gelatinase localization or expression. Since we primarily observed co-localization of MMP-2 with ISZ and increased activation form of MMP-2 was detected in OGD neurons, we hypothesize that MMP-2 is the major contributor to the observed nuclear gelatinase activity at this time point. However, although MMP-2 may account for most of the nuclear gelatinase activity, the overall increase in nuclear MMP-9 level was significantly greater than that observed for MMP-2. These results specifically establish MMP-2 and -9 as major intranuclear proteolytic activities in post-OGD neurons.

Since apoptotic neurons co-localized with intracellular gelatinase activity, these results suggested that gelatinase activity in neurons might be complicit in the induction of apoptosis during reoxygenation after OGD. Remarkably, specific inhibition of gelatinase activity during OGD and reoxygenation was exceptionally neuroprotective and reduced neuronal death by greater than 50%, suggesting a major role for intracellular gelatinases in neuronal cell death. To test the possibility that neuronal death after OGD might be due to variations in extracellular gelatinase activity, we measured gelatinase levels in culture medium of control and OGD-treated neurons with and without MMP-2/9 inhibitor treatment. No change in extracellular gelatinase activity was observed under any condition. These results suggest that the increase in gelatinase activity induced by OGD is primarily intracellular at 24-h reoxygenation. Since early induction of gelatinases associated with nuclear condensation and apoptosis was primarily nuclear, our results suggest that nuclear gelatinases are associated with neuronal apoptosis after OGD. However, we cannot exclude a possible

contribution by cytoplasmic or membrane-bound gelatinases to neuronal apoptotic cell death pathways.

Accumulation of oxidative DNA damage, including 8-oxoguanine and abasic sites, is associated with ischemia/reperfusion injury and neurodegeneration. Oxidative DNA damage is repaired primarily by the BER pathway. PARP1 plays an integral role in BER where it binds to abasic sites and single-strand breaks and functions as a scaffolding protein directing repair enzymes to the lesion site (Almeida and Sobol, 2007). Alternatively, overwhelming DNA damage leads to PARP1 overactivation, cellular energy depletion, and ADP-ribosylation of numerous proteins, including PARP1. PAR produced by the enzymatic activity of PARP1 can enter mitochondria and promote the nuclear translocation of apoptosis inducing factor (AIF) leading to caspase-independent cell death (Hassa, 2009). Thus, PARP1 may have antagonist effects on cell survival, depending upon the extent of DNA damage incurred. A role for PARP1 overactivation in neuronal death is supported by studies demonstrating the neuroprotective effects of PARP1 inhibitors after stroke (Moroni and Chiarugi, 2009). However, some PARP1 inhibitors also inhibit MMP-2 (Nicolescu et al., 2009). Thus, the neuroprotective effects of PARP inhibitors may in part be mediated by inhibition of MMP-2. While the decreased level of PAR we observed after OGD might favor cell survival, the decreased level of PARP1 enzyme might impair DNA repair function and promote DNA damage and cell death. This latter possibility is supported by our observations that decreased PARP1 level and activity were associated with elevated DNA damage and apoptosis after OGD and is consistent with our *in vivo* study (Yang et al., 2010).

XRCC1 interacts with PARP1, directly with damaged DNA, and with other components of BER, including glycosylases, polymerases, and ligases to orchestrate the formation of repair complexes at lesion sites (Almeida and Sobol, 2007). Studies have shown an association between the loss of XRCC1 and the induction of apoptosis in animal models of stroke (Fujimura et al., 1999; Yang et al., 2010). In the present study, we report that the decrease in XRCC1 in neurons occurs by a gelatinase-associated mechanism, in confirmation of our earlier observations in an animal stroke model. We further show that the loss of XRCC1 is associated with induction of intrinsic neuronal apoptosis and can be prevented by treatment with a specific MMP-2/9 inhibitor.

The level of OGG1, the major 8-oxoguanine repair activity, was significantly decreased after OGD. The loss of OGG1 was not significantly rescued by MMP inhibitor treatment and suggests the involvement of other proteases in the degradation of OGG1, such as calpain, which is upregulated in apoptotic neurons exposed to OGD and mediates cleavage of PARP1 and OGG1 in neurons and other cells (Boland and Campbell, 2003; Cao et al., 2007; Hill et al., 2008). The observed increase in 8-oxo-dG in DNA may be due to the loss of OGG1. However, with MMP inhibitor treatment, the level of 8-oxo-dG in DNA after OGD was similar to normoxic controls, although the level of OGG1 remained low. This could be due to posttranslational modifications of DNA repair enzymes, such as OGG1, that could modify repair activity independent of protein level. For instance, Cdk4 phosphorylation of OGG1 was shown to increase OGG1 strand incision activity 2.5-fold at 8-oxo-dG lesions (Hu et al., 2005). While we observed no significant change in the level of APE1 at 24-h reoxygenation after OGD, post-ischemic phosphorylation of DNA polymerase

β (pol β) and APE1 was shown to downregulate BER activity without a significant change in protein levels (Luo et al., 2007). Thus, BER activity in neurons appears to be regulated at multiple levels, including proteolysis of BER proteins by gelatinases. Alternatively, gelatinases may directly influence the formation of reactive oxygen species and oxidative DNA damage through an unknown mechanism.

We show that neuronal death after OGD is mediated by the involvement of MMP-2 and -9 in an intrinsic cell death pathway, in addition to the previously reported extrinsic pathway involving gelatinases produced by non-neuronal cells. The elucidation of the relative contribution and importance of each pathway in neuronal death after stroke, along with a more complete understanding of the roles of changes in MMP-2 and -9 levels, activity, and compartmentalization in neuronal death are warranted and may lead to novel molecular targets for therapeutic intervention. The protection of neurons by a specific inhibitor of MMP-2 and -9 that we observed *in vitro* suggests that the protective effects of broad-spectrum MMP inhibitors *in vivo* after stroke may be in large part mediated through the inhibition of gelatinases. Our results show that changes in the intracellular localization and activity of gelatinases are involved in intrinsic neuronal apoptosis after OGD and suggest that early inhibition of gelatinases may represent an effective neuroprotective therapy for stroke.

Acknowledgements

This work was supported by Beginning Grants-in-Aid from the American Heart Association (0765473Z and 10BGIA4310034) to YY and a National Institutes of Health (NIH)-supported Centers of Biomedical Research Excellence (COBRE) pilot grant from the University of New Mexico to YY. Confocal images were generated in the University of New Mexico & Cancer Center Fluorescence Microscopy Shared Resource, funded as detailed on: www.hsc.unm.edu/crtc/microscopy/facility.html.

Abbreviations

8-oxo-dG	8-hydroxy-2′-dexoguanine
BBB	blood–brain barrier
BER	base excision repair
Cy3	Cyanine 3
DAPI	4′-6-diamidino-2-phenylindole
DMSO	dimethyl sulfoxide
dUTP	deoxyuridine triphosphate
FBS	fetal bovine serum
FITC	fluorescein isothiocyanate
HBSS	Hank’s buffered saline solution
ISZ	In situ zymography
MCAO	middle cerebral artery occlusion

MMP	matrix metalloproteinase
OGD	oxygen–glucose deprivation
PAR	poly ADP-ribose
PARP1	poly-ADP ribose polymerase
PBS	phosphate-buffered saline
PVDF	polyvinylidene fluoride
TUNEL	terminal deoxynucleotidyl transferase-mediated dUTP nick end labeling
XRCC1	X-ray cross-complementary factor 1.

REFERENCES

Ali MA, Schulz R. Activation of MMP-2 as a key event in oxidative stress injury to the heart. Front Biosci. 2009; 14:699–716.

Almeida KH, Sobol RW. A unified view of base excision repair: lesion-dependent protein complexes regulated by post-translational modification. DNA Repair (Amst). 2007; 6:695–711. [PubMed: 17337257]

Amantea D, Corasaniti MT, Mercuri NB, Bernardi G, Bagetta G. Brain regional and cellular localization of gelatinase activity in rat that have undergone transient middle cerebral artery occlusion. Neuroscience. 2008; 152:8–17. [PubMed: 18255236]

Amantea D, Russo R, Gliozzi M, Fratto V, Berliocchi L, Bagetta G, Bernardi G, Corasaniti MT. Early upregulation of matrix metalloproteinases following reperfusion triggers neuroinflammatory mediators in brain ischemia in rat. Int Rev Neurobiol. 2007; 82:149–169. [PubMed: 17678960]

Asahi M, Asahi K, Jung JC, del Zoppo GJ, Fini ME, Lo EH. Role for matrix metalloproteinase 9 after focal cerebral ischemia: effects of gene knockout and enzyme inhibition with BB-94. J Cereb Blood Flow Metab. 2000; 20:1681–1689. [PubMed: 11129784]

Boland B, Campbell V. Beta-Amyloid (1–40)-induced apoptosis of cultured cortical neurones involves calpain-mediated cleavage of poly-ADP-ribose polymerase. Neurobiol Aging. 2003; 24:179–186. [PubMed: 12493564]

Broughton BR, Reutens DC, Sobey CG. Apoptotic mechanisms after cerebral ischemia. Stroke. 2009; 40:e331–e339. [PubMed: 19182083]

Candelario-Jalil E, Thompson J, Taheri S, Grossetete M, Adair JC, Edmonds E, Prestopnik J, Wills J, Rosenberg GA. Matrix metalloproteinases are associated with increased blood-brain barrier opening in vascular cognitive impairment. Stroke. 2011; 42:1345–1350. [PubMed: 21454822]

Candelario-Jalil E, Yang Y, Rosenberg GA. Diverse roles of matrix metalloproteinases and tissue inhibitors of metalloproteinases in neuroinflammation and cerebral ischemia. Neuroscience. 2009; 158:983–994. [PubMed: 18621108]

Cao G, Xing J, Xiao X, Liou AK, Gao Y, Yin XM, Clark RS, Graham SH, Chen J. Critical role of calpain I in mitochondrial release of apoptosis-inducing factor in ischemic neuronal injury. J Neurosci. 2007; 27:9278–9293. [PubMed: 17728442]

Cauwe B, Opdenakker G. Intracellular substrate cleavage: a novel dimension in the biochemistry, biology and pathology of matrix metalloproteinases. Crit Rev Biochem Mol Biol. 2011; 45:351–423. [PubMed: 20812779]

Choi DH, Kim EM, Son HJ, Joh TH, Kim YS, Kim D, Flint Beal M, Hwang O. A novel intracellular role of matrix metalloproteinase-3 during apoptosis of dopaminergic cells. J Neurochem. 2008; 106:405–415. [PubMed: 18397366]

Copin JC, Goodyear MC, Gidday JM, Shah AR, Gascon E, Dayer A, Morel DM, Gasche Y. Role of matrix metalloproteinases in apoptosis after transient focal cerebral ischemia in rats and mice. Eur J Neurosci. 2005; 22:1597–1608. [PubMed: 16197500]

Cuadrado E, Rosell A, Borrell-Pages M, Garcia-Bonilla L, Hernandez-Guillamon M, Ortega-Aznar A, Montaner J. Matrix metalloproteinase-13 is activated and is found in the nucleus of neural cells after cerebral ischemia. J Cereb Blood Flow Metab. 2009; 29:398–410. [PubMed: 18985055]

Cunningham LA, Wetzel M, Rosenberg GA. Multiple roles for MMPs and TIMPs in cerebral ischemia. Glia. 2005; 50:329–339. [PubMed: 15846802]

Fujimura M, Morita-Fujimura Y, Sugawara T, Chan PH. Early decrease of XRCC1, a DNA base excision repair protein, may contribute to DNA fragmentation after transient focal cerebral ischemia in mice. Stroke. 1999; 30:2456–2462. [PubMed: 10548684]

Gasche Y, Copin JC, Sugawara T, Fujimura M, Chan PH. Matrix metalloproteinase inhibition prevents oxidative stress-associated blood-brain barrier disruption after transient focal cerebral ischemia. J Cereb Blood Flow Metab. 2001; 21:1393–1400. [PubMed: 11740200]

Gu Z, Cui J, Brown S, Fridman R, Mobashery S, Strongin AY, Lipton SA. A highly specific inhibitor of matrix metalloproteinase-9 rescues laminin from proteolysis and neurons from apoptosis in transient focal cerebral ischemia. J Neurosci. 2005; 25:6401–6408. [PubMed: 16000631]

Gu Z, Kaul M, Yan B, Kridel SJ, Cui J, Strongin A, Smith JW, Liddington RC, Lipton SA. S-nitrosylation of matrix metalloproteinases: signaling pathway to neuronal cell death. Science. 2002; 297:1186–1190. [PubMed: 12183632]

Gueye Y, Ferhat L, Sbai O, Bianco J, Ould-Yahoui A, Bernard A, Charrat E, Chauvin JP, Risso JJ, Feron F, Rivera S, Khrestchatisky M. Trafficking and secretion of matrix metalloproteinase-2 in olfactory ensheathing glial cells: a role in cell migration? Glia. 2011; 59:750–770. [PubMed: 21360755]

Hassa PO. The molecular “Jekyll and Hyde” duality of PARP1 in cell death and cell survival. Front Biosci. 2009; 14:72–111.

Hill JW, Hu JJ, Evans MK. OGG1 is degraded by calpain following oxidative stress and cisplatin exposure. DNA Repair (Amst). 2008; 7:648–654. [PubMed: 18294929]

Hu J, Imam SZ, Hashiguchi K, de Souza-Pinto NC, Bohr VA. Phosphorylation of human oxoguanine DNA glycosylase (alpha-OGG1) modulates its function. Nucleic Acids Res. 2005; 33:3271–3282. [PubMed: 15942030]

Jin R, Yang G, Li G. Molecular insights and therapeutic targets for blood-brain barrier disruption in ischemic stroke: critical role of matrix metalloproteinases and tissue-type plasminogen activator. Neurobiol Dis. 2010; 38:376–385. [PubMed: 20302940]

Katsu M, Niizuma K, Yoshioka H, Okami N, Sakata H, Chan PH. Hemoglobin-induced oxidative stress contributes to matrix metalloproteinase activation and blood-brain barrier dysfunction in vivo. J Cereb Blood Flow Metab. 2010; 30:1939–1950. [PubMed: 20354546]

Kauppinen TM, Swanson RA. Poly(ADP-ribose) polymerase-1 promotes microglial activation, proliferation, and matrix metalloproteinase-9-mediated neuron death. J Immunol. 2005; 174:2288–2296. [PubMed: 15699164]

Koistinaho M, Malm TM, Kettunen MI, Goldsteins G, Starckx S, Kauppinen RA, Opdenakker G, Koistinaho J. Minocycline protects against permanent cerebral ischemia in wild type but not in matrix metalloprotease-9-deficient mice. J Cereb Blood Flow Metab. 2005; 25:460–467. [PubMed: 15674236]

Kwan JA, Schulze CJ, Wang W, Leon H, Sariahmetoglu M, Sung M, Sawicka J, Sims DE, Sawicki G, Schulz R. Matrix metalloproteinase-2 (MMP-2) is present in the nucleus of cardiac myocytes and is capable of cleaving poly (ADP-ribose) polymerase (PARP) in vitro. Faseb J. 2004; 18:690–692. [PubMed: 14766804]

Liu W, Hendren J, Qin XJ, Shen J, Liu KJ. Normobaric hyperoxia attenuates early blood-brain barrier disruption by inhibiting MMP-9-mediated occludin degradation in focal cerebral ischemia. J Neurochem. 2009; 108:811–820. [PubMed: 19187098]

Luo Y, Ji X, Ling F, Li W, Zhang F, Cao G, Chen J. Impaired DNA repair via the base-excision repair pathway after focal ischemic brain injury: a protein phosphorylation-dependent mechanism reversed by hypothermic neuroprotection. Front Biosci. 2007; 12:1852–1862. [PubMed: 17127426]

Mannello F, Medda V. Nuclear localization of Matrix metalloproteinases. Prog Histochem Cytochem. 2012; 47:27–58. [PubMed: 22226510]

McColl BW, Rothwell NJ, Allan SM. Systemic inflammation alters the kinetics of cerebrovascular tight junction disruption after experimental stroke in mice. J Neurosci. 2008; 28:9451–9462. [PubMed: 18799677]

Moroni F, Chiarugi A. Post-ischemic brain damage: targeting PARP-1 within the ischemic neurovascular units as a realistic avenue to stroke treatment. FEBS J. 2009; 276:36–45. [PubMed: 19087198]

Neumann J, Sauerzweig S, Ronicke R, Gunzer F, Dinkel K, Ullrich O, Gunzer M, Reymann KG. Microglia cells protect neurons by direct engulfment of invading neutrophil granulocytes: a new mechanism of CNS immune privilege. J Neurosci. 2008; 28:5965–5975. [PubMed: 18524901]

Nicolescu AC, Holt A, Kandasamy AD, Pacher P, Schulz R. Inhibition of matrix metalloproteinase-2 by PARP inhibitors. Biochem Biophys Res Commun. 2009; 387:646–650. [PubMed: 19619515]

Romanic AM, White RF, Arleth AJ, Ohlstein EH, Barone FC. Matrix metalloproteinase expression increases after cerebral focal ischemia in rats: inhibition of matrix metalloproteinase-9 reduces infarct size. Stroke. 1998; 29:1020–1030. [PubMed: 9596253]

Rosenberg GA, Cunningham LA, Wallace J, Alexander S, Estrada EY, Grossetete M, Razhagi A, Miller K, Gearing A. Immunohistochemistry of matrix metalloproteinases in reperfusion injury to rat brain: activation of MMP-9 linked to stromelysin-1 and microglia in cell cultures. Brain Res. 2001; 893:104–112. [PubMed: 11222998]

Rosenberg GA, Yang Y. Vasogenic edema due to tight junction disruption by matrix metalloproteinases in cerebral ischemia. Neurosurg Focus. 2007; 22:E4. [PubMed: 17613235]

Si-Tayeb K, Monvoisin A, Mazzocco C, Lepreux S, Decossas M, Cubel G, Taras D, Blanc JF, Robinson DR, Rosenbaum J. Matrix metalloproteinase 3 is present in the cell nucleus and is involved in apoptosis. Am J Pathol. 2006; 169:1390–1401. [PubMed: 17003494]

Wakisaka Y, Chu Y, Miller JD, Rosenberg GA, Heistad DD. Spontaneous intracerebral hemorrhage during acute and chronic hypertension in mice. J Cereb Blood Flow Metab. 2010; 30:56–69. [PubMed: 19724290]

Walker EJ, Rosenberg GA. Divergent role for MMP-2 in myelin breakdown and oligodendrocyte death following transient global ischemia. J Neurosci Res. 2010; 88:764–773. [PubMed: 19830840]

Yang Y, Candelario-Jalil E, Thompson JF, Cuadrado E, Estrada EY, Rosell A, Montaner J, Rosenberg GA. Increased intranuclear matrix metalloproteinase activity in neurons interferes with oxidative DNA repair in focal cerebral ischemia. J Neurochem. 2010; 112:134–149. [PubMed: 19840223]

Yang Y, Estrada EY, Thompson JF, Liu W, Rosenberg GA. Matrix metalloproteinase-mediated disruption of tight junction proteins in cerebral vessels is reversed by synthetic matrix metalloproteinase inhibitor in focal ischemia in rat. J Cereb Blood Flow Metab. 2007; 27:697–709. [PubMed: 16850029]

Yang Y, Jalal FY, Thompson JF, Walker EJ, Candelario-Jalil E, Li L, Reichard RR, Ben C, Sang QX, Cunningham LA, Rosenberg GA. Tissue inhibitor of metalloproteinases-3 mediates the death of immature oligodendrocytes via TNF-alpha/TACE in focal cerebral ischemia in mice. J Neuroinflammation. 2011; 8:108. [PubMed: 21871134]

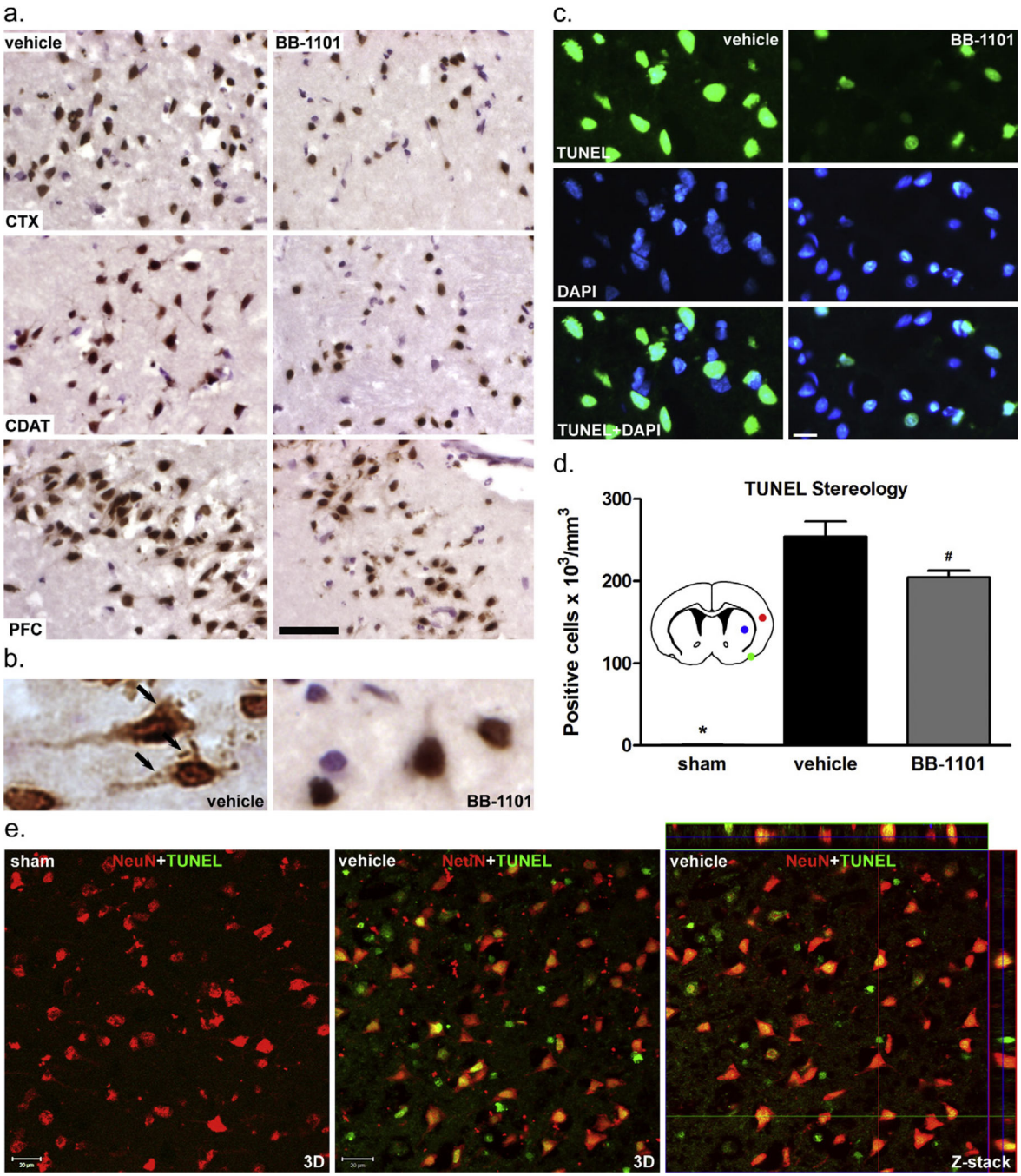

Fig. 1.

Involvement of MMPs in apoptotic cell death in rat brain at 48-h post-ischemic reperfusion. (a) Representative DAB-TUNEL staining showing increased TUNEL-positive cells in saline vehicle-treated compared to BB-1101-treated cortex (CTX), caudate (CDAT), and piriform cortex (PFC). Scale bar=50 μm. (b) Apoptotic body-like staining in the cytoplasm of apoptotic neurons in vehicle-treated infarct PFC (arrows). (c) Representative TUNEL-fluorescence and DAPI-nuclear staining showing increased DNA fragmentation in ischemic infarct cortex without BB-1101 treatment. Scale bar=20 μm. (d) TUNEL-positive cell

stereology in whole ischemic hemispheres. A significant increase in TUNEL-positive cells ($\times 10^3/mm^3$) was observed in ischemic hemispheres both with and without BB-1101 treatment compared to sham animals (*), $p < 0.01$. Sham group $n = 3$, vehicle group $n = 5$, BB-1101 group $n = 4$. Significantly less TUNEL-positive cells were detected in the BB-1101-treated ischemic hemispheres (#) compared to vehicle, $p < 0.05$. Inset diagram, stereological analysis of the entire ischemic (right) hemisphere was done over a distance of 3.0, 1.5 mm rostral and caudal to the bregma. Images in panel (a) were obtained from the infarct areas indicated (red, cortex; blue, caudate; green, piriform cortex). (e) Representative confocal images of double-staining for NeuN and TUNEL show that most TUNEL-positive cells are neurons in ischemic infarct cortex at 48-h reperfusion. Scale bar = 20 μm.

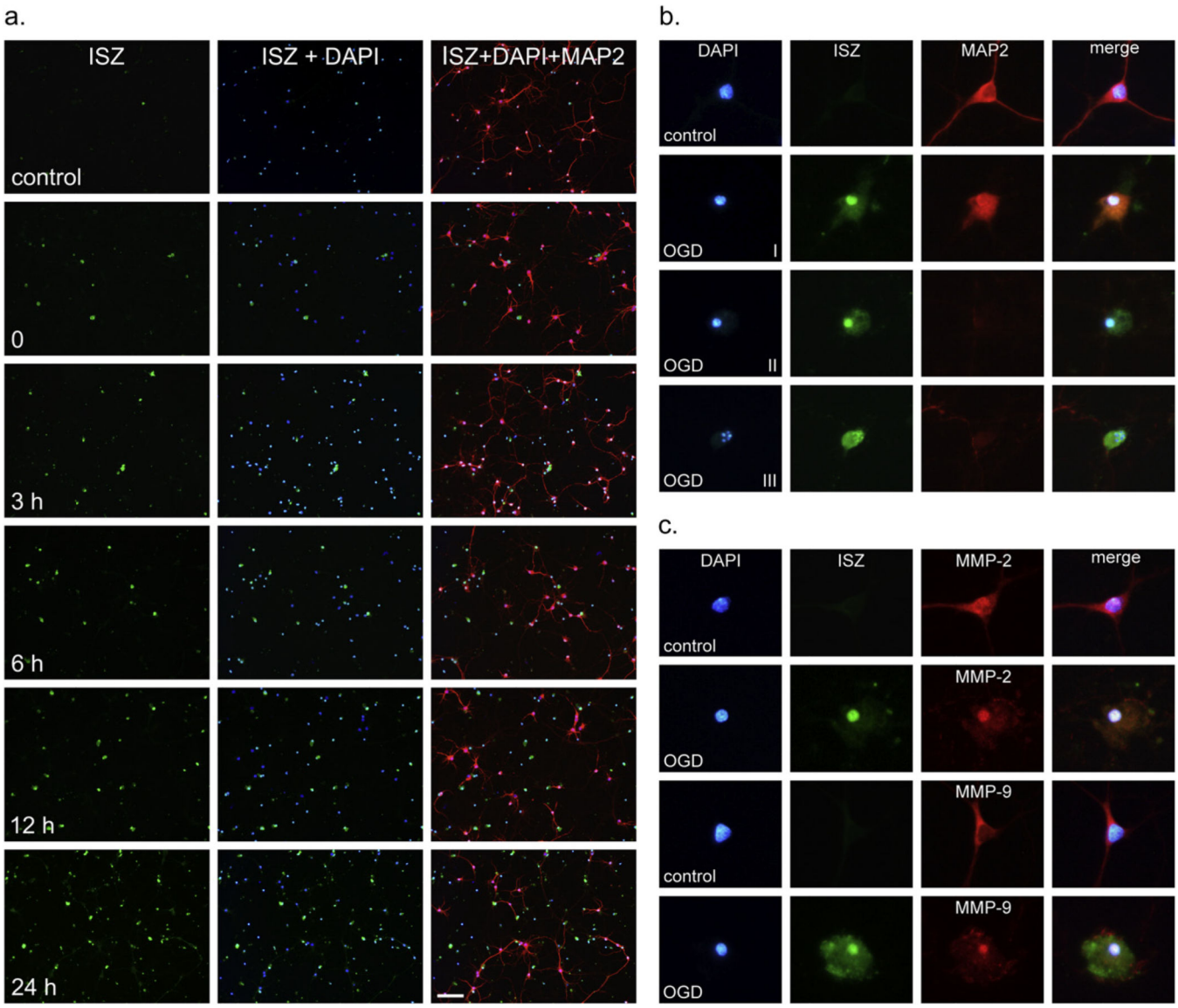

Fig. 2.

Induction of gelatinase activity and nuclear localization of MMP-2 and -9 in cortical neurons after OGD. (a) *In situ* zymography (ISZ) was performed on living neurons after 0, 3-, 6-, 12-, and 24-h reoxygenation as described in Experimental Procedures. ISZ-positive cells are stained green in column 1, nuclei are stained blue with DAPI in column 2, and neurons are identified with a neuron-specific marker (anti-MAP2 polyclonal antibody) in column 3. Superimposition of ISZ, DAPI, and MAP2 shows gelatinase activity in neurons. Scale bar = 100 μm. (b) The stages of gelatinase induction associated with apoptosis are shown. Stage I, early apoptosis with nuclear condensation, strong nuclear gelatinase activity, and retraction of cellular processes. Stage II, mid-stage apoptosis with further condensation of the nucleus, collapse of the cytoskeleton, and loss of MAP2 staining. Stage III, late-stage apoptosis with clear nuclear fragmentation and intense uniform gelatinase activity throughout the cell. (c) Using immunocytochemistry, MMP-2 was detected in nuclei in both control and OGD-treated cells and increased in the nucleus 24 h after OGD. MMP-9 could not be detected in

the nucleus of control cells by immunocytochemistry but was detectable in neuronal nuclei after OGD.

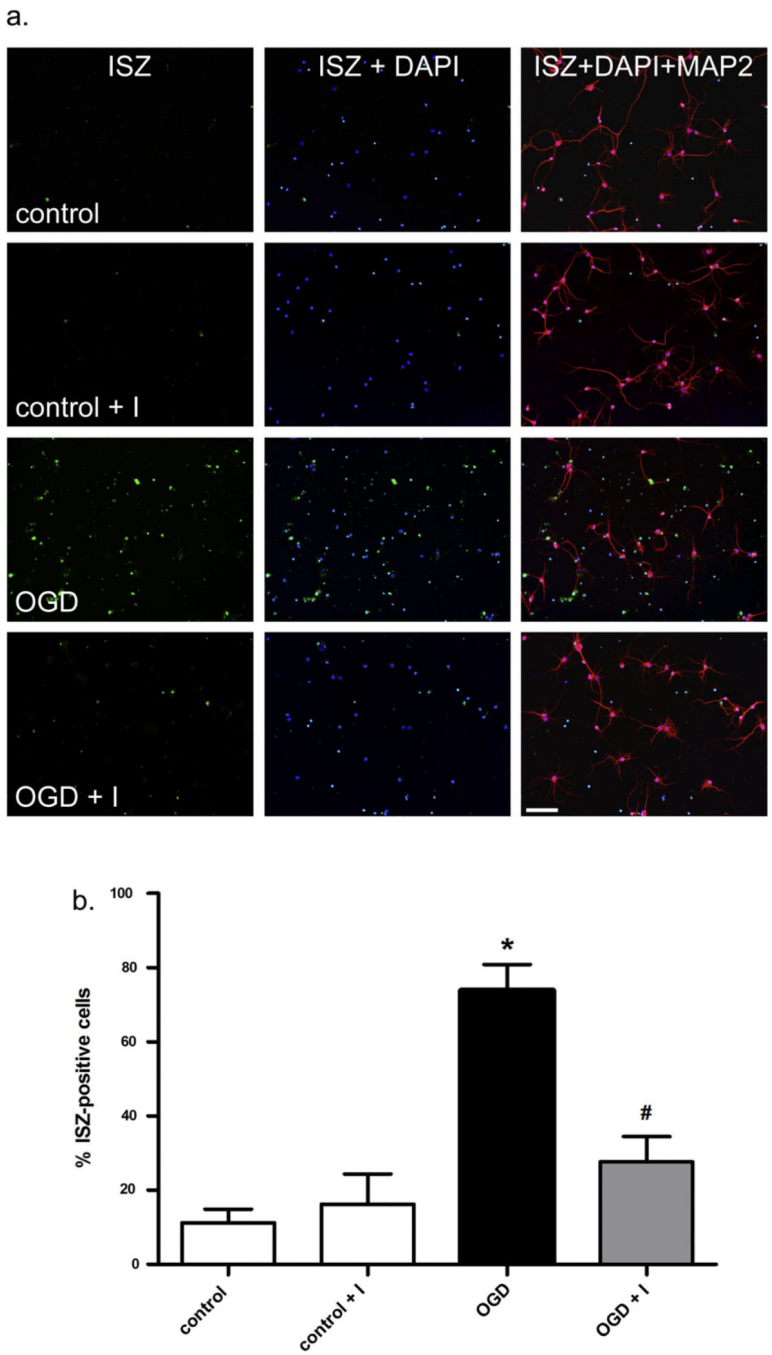

Fig. 3.

Gelatinase activity after OGD is inhibited by MMP-2/9 inhibitor II. The percentage of gelatinase-positive neurons was measured 24 h after OGD. (a) Both control and OGD experiments were performed with and without treatment with MMP-2/9 inhibitor II. Scale bar = 100 μm. The percentage of cells with gelatinase activity for each condition was determined from 4 experiments and results are shown graphically in (b) A statistically significant ($p < 0.01$) difference in the percent of ISZ-positive cells between control and OGD-treated cells (*) and between OGD and OGD plus inhibitor was observed (#).

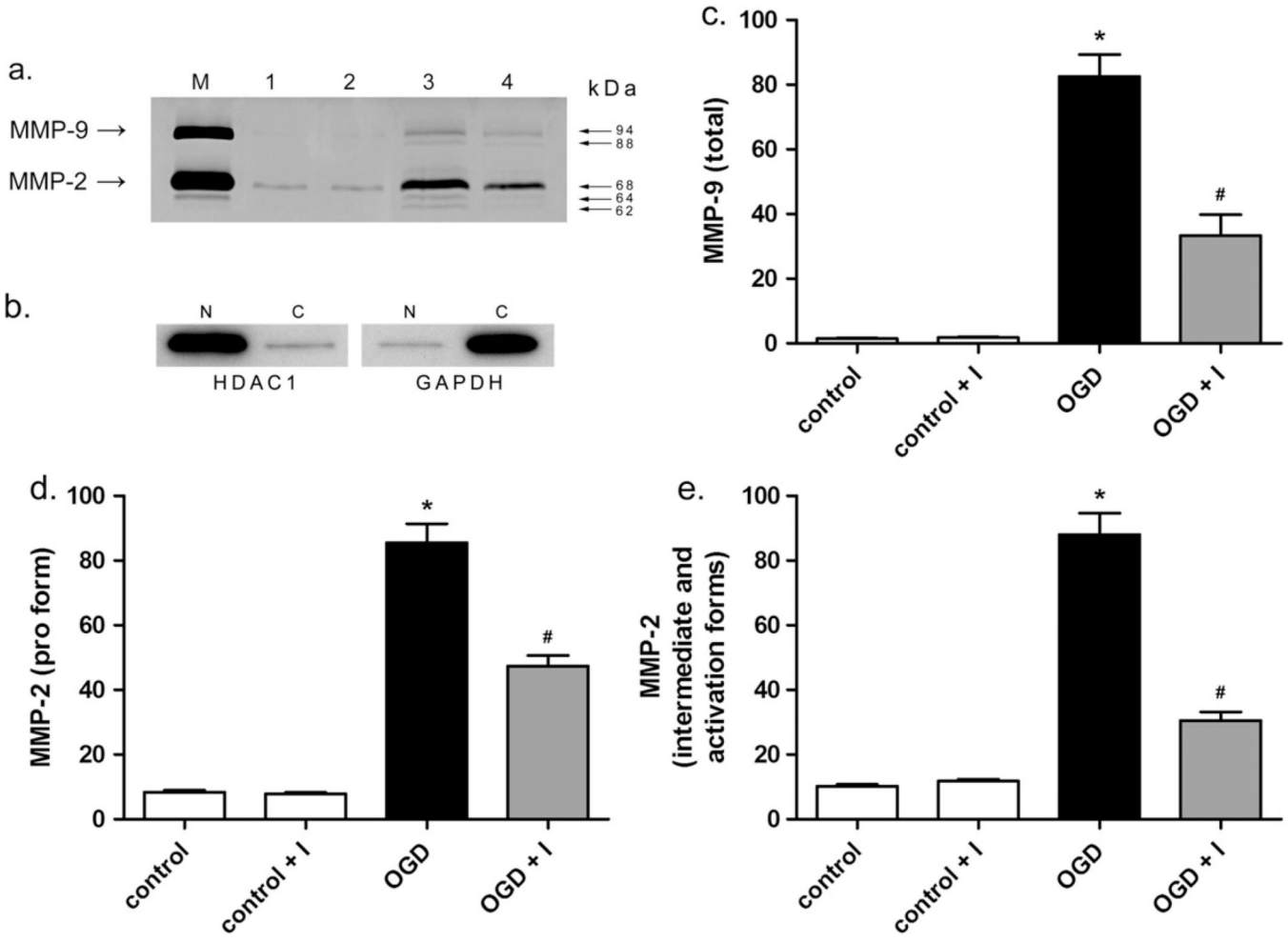

Fig. 4.

Measurement of MMP-2 and MMP-9 levels in neuronal nuclei after OGD. The levels of MMP-2 and -9 in the nuclei of neurons were evaluated by gelatin zymography 24 h after OGD or mock treatment with or without MMP-2/9 inhibitor II. In agreement with immunocytochemistry (Fig. 2c), MMP-9 was undetectable in the nucleus by gelatin zymography in control cells and was elevated following OGD. MMP-2 was observed in the nucleus in control cells and was elevated after OGD. (a) Gelatin zymogram showing MMP-2 and -9 levels (photographically negative). M, HT1080 culture medium standard for MMP-2 and -9. Lane 1, control, lane 2, control plus inhibitor, lane 3, OGD, lane 4, OGD plus inhibitor. Molecular weights indicate MMP-9 glycosylated and pro forms, 94 and 88 kDa, respectively, and MMP-2 pro, intermediate, and activation forms, 68, 64, and 62 kDa, respectively. (b) Control Western blot showing fractionation of nuclear and cytoplasmic proteins. Five micrograms neuronal nuclear (N) and cytoplasmic (C) extract were immunoblotted with antibody to HDAC1, nuclear protein histone deacetylase 1, left panel, or cytoplasmic protein glyceraldehyde 3-phosphate dehydrogenase, GAPDH, right panel. (c–e) Graphical representations of relative MMP-9 and -2 levels in nuclear extracts shown as the mean and standard deviation of 4 independent experiments. Units are arbitrary. (c) Total MMP-9 level. (d and e) Levels of pro and intermediate and activation forms of MMP-2,

respectively. Asterisks indicate statistically significant differences between control and OGD, while pound signs indicate significant differences between OGD and OGD plus inhibitor, $p < 0.01$.

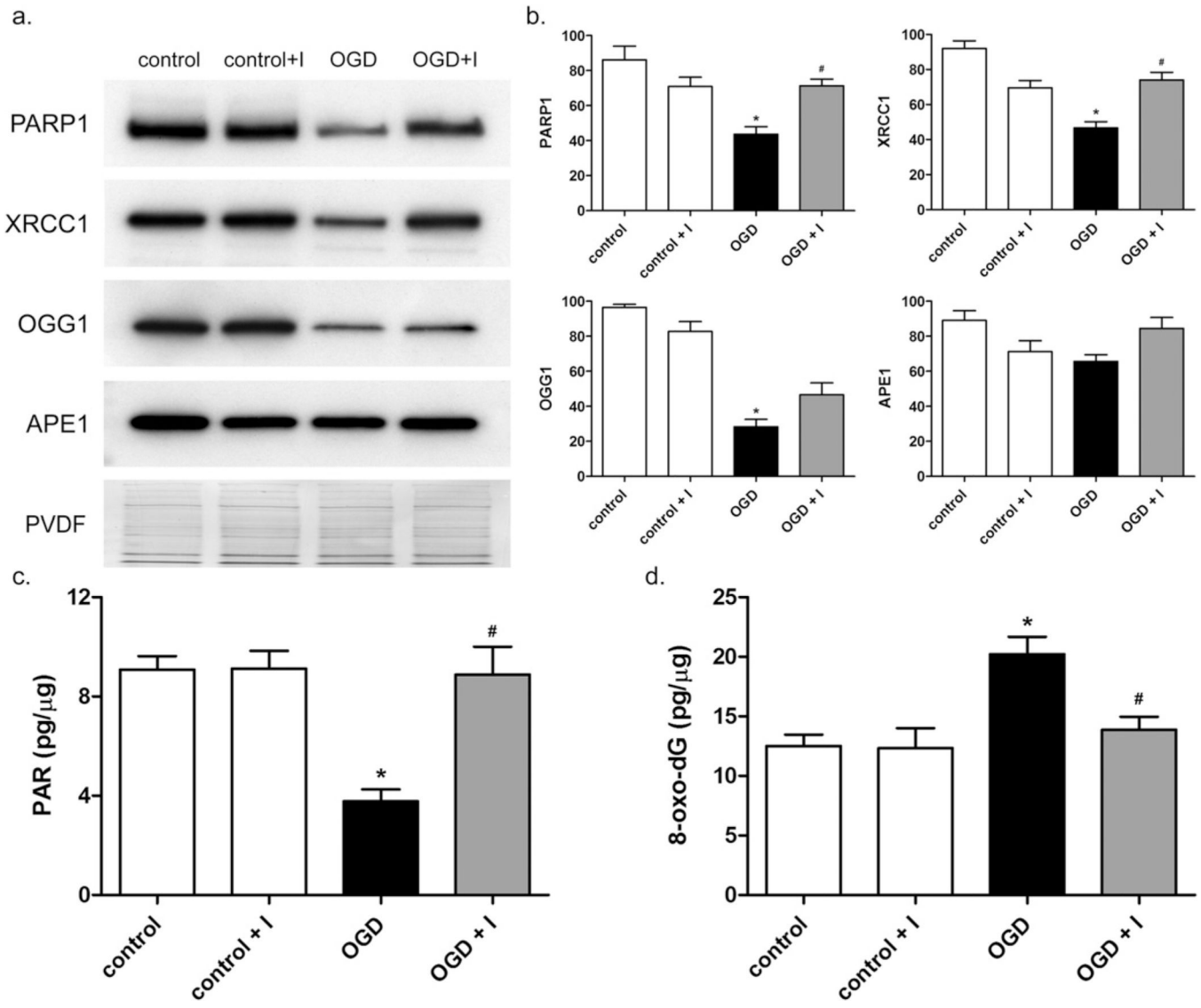

Fig. 5.

Decreased levels of DNA repair proteins and measurement of oxidative DNA damage and PARP1 activity in neuronal nuclei after OGD. (a) The levels of DNA repair proteins PARP1, XRCC1, OGG1, and APE1 in nuclear extracts of neurons exposed to control (lane 1), control plus inhibitor (lane 2), OGD (lane 3), or OGD plus inhibitor (lane 4) conditions were measured by Western blot. (b) Graphical representation of normalized relative levels of DNA repair proteins. Units are arbitrary. For PARP1 and XRCC1, protein levels were significantly lower in OGD-treated cells compared to controls (*), and significantly higher in OGD plus inhibitor compared to OGD (#), $p < 0.01$. OGG1 significantly decreased after OGD (*) and no significant changes in APE1 were observed. (c) Level of PAR present in the nucleus of neurons in pg PAR per μg nuclear extract. OGD caused a statistically significant decrease in nuclear PAR level compared to control cells (*), $p < 0.01$. In the presence of MMP-2/9 inhibitor II, a significant difference in nuclear PAR levels between OGD and OGD plus inhibitor was observed (#), $p < 0.01$. (d) After OGD and 24-h

reoxygenation, 8-oxo-dG in genomic DNA (pg per μg DNA) was measured as described in Experimental Procedures. 8-oxo-dG was significantly elevated in OGD-treated cells compared to controls (*), $p < 0.01$, and significantly lower in OGD plus inhibitor compared to OGD (#), $p < 0.05$. Results are means and standard deviations from 4 independent experiments.

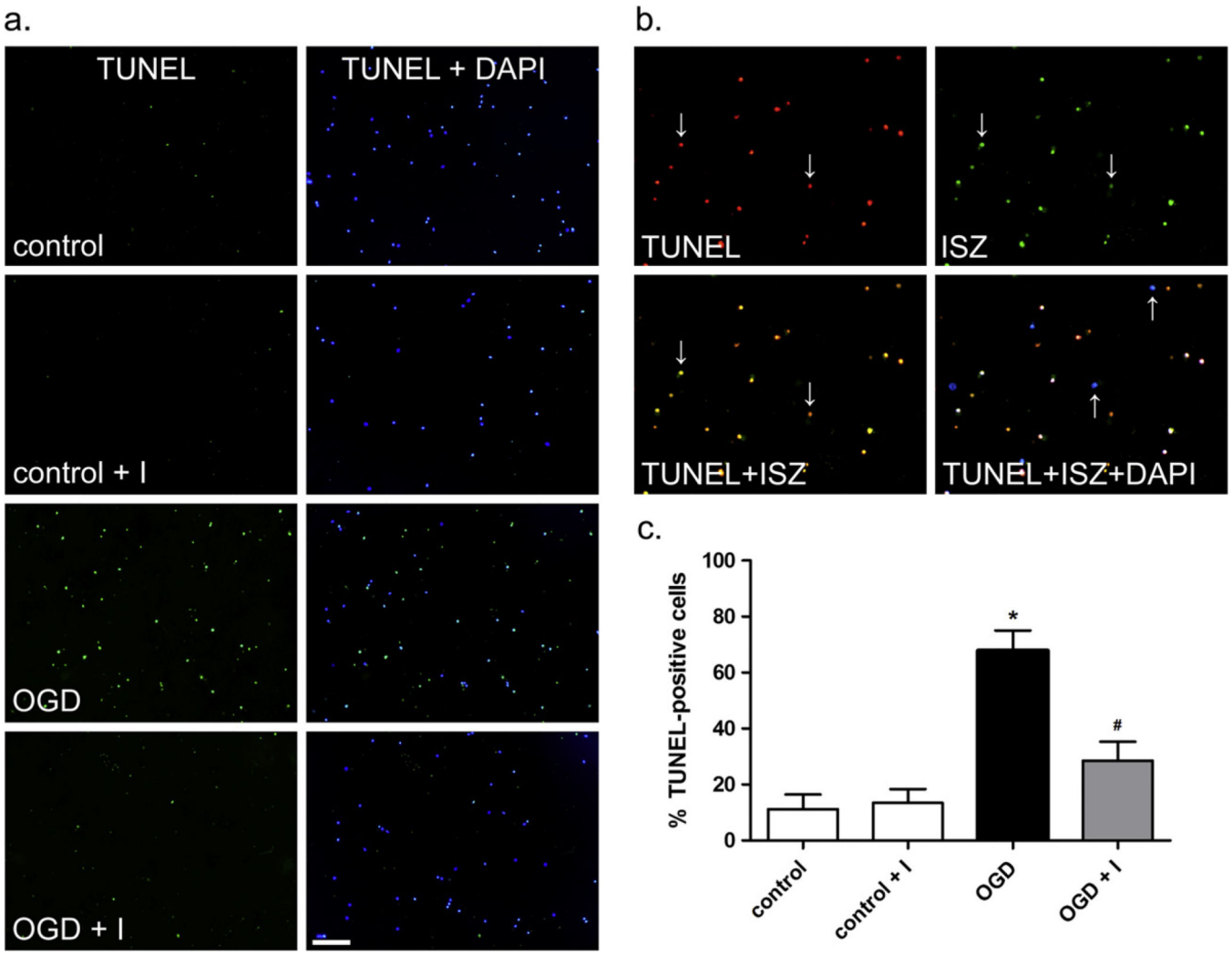

Fig. 6.

Apoptosis and co-localization of apoptosis and ISZ in neurons. Apoptosis in neurons was measured by TUNEL assay after OGD and 24-h reoxygenation as described in Experimental Procedures. (a) Apoptotic cells are labeled green and superimposed with blue DAPI-stained nuclei. Scale bar=100 μm. (b) Co-localization of TUNEL and ISZ. Apoptotic cells (red) are superimposed with ISZ (green). When superimposed, cells positive for both TUNEL and ISZ appear yellow (indicated by down arrows) while healthy cells (blue) are stained with DAPI alone (indicated by up arrows). (c) Percent apoptotic cells for each condition as determined by counting cells from 4 independent experiments. Results are shown as means with standard deviation. A statistically significant difference in apoptosis was observed between control and OGD (*) and OGD plus inhibitor and OGD (#), $p < 0.01$.

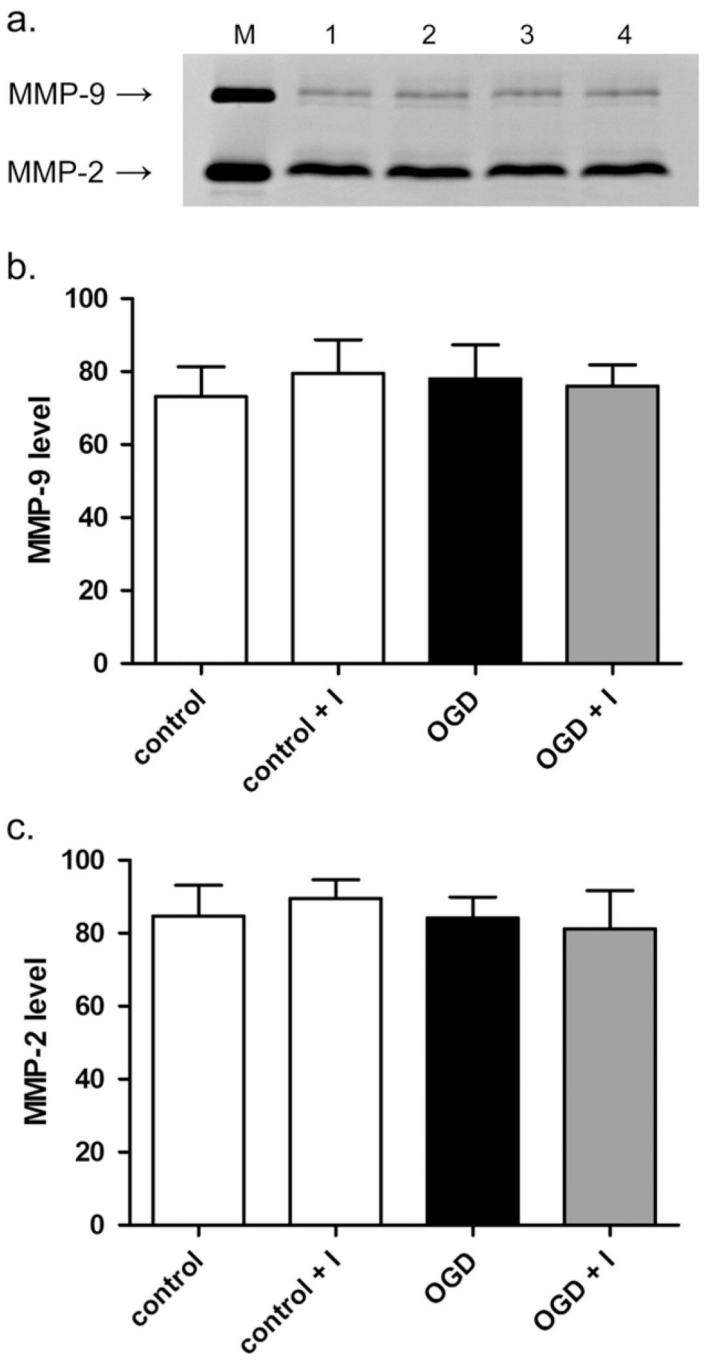

Fig. 7.

Measurement of gelatinase levels in neuronal culture medium after OGD. Gelatinase levels in culture medium after OGD or mock treatment with or without MMP-2/9 inhibitor II were measured by gelatin zymography. (a) Gelatin zymogram showing MMP-2 and -9 levels (photographically negative). M, HT1080 culture medium standard for MMP-2 and -9. Lane 1, control, lane 2, control plus inhibitor, lane 3, OGD, lane 4, OGD plus inhibitor. (b and c)

Graphical representations of relative MMP-9 and -2 levels in culture medium shown as the mean and standard deviation of 4 independent experiments. Units are arbitrary.